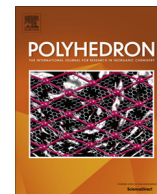




Contents lists available at ScienceDirect

Polyhedron

journal homepage: www.elsevier.com/locate/poly

Nanoscale Pd-based catalysts for selective oxidation of glycerol with molecular oxygen: Structure–activity correlations

Sharifah Bee Abd Hamid ^{a,*}, Norfatehah Basiron ^a, Wageeh A. Yehye ^a, Putla Sudarsanam ^b, Suresh K. Bhargava ^b

^a Nanotechnology & Catalysis Research Centre (NANOCAT), University of Malaya, 50603 Kuala Lumpur, Malaysia

^b Centre for Advanced Materials and Industrial Chemistry (CAMIC), School of Science, RMIT University, Melbourne, VIC 3001, Australia

ARTICLE INFO

Article history:

Received 13 May 2016

Accepted 19 July 2016

Available online xxx

Keywords:

Palladium catalysts

Hydrotalcite

Activated carbon

Glycerol oxidation

Glyceric acid

ABSTRACT

This work investigates selective oxidation of glycerol with molecular oxygen, one of the viable routes to obtain value-added products from bio-glycerol, using nanosized Pd-based catalysts. For this, three types of 1 wt.% Pd catalysts supported on activated carbon (Ac), hydrotalcite (HTc), and activated carbon–hydrotalcite composite (Ac–HTc) were prepared. The physicochemical properties of the catalysts are characterized using various techniques, such as XRD, BET, XRF, H₂-TPR, CO₂-TPD, and TEM. The TEM images reveal the formation of Pd nanoparticles with an average diameter of 9.01, 9.10, and 11.16 nm on the surface of HTc, Ac, and Ac–HTc supports, respectively. The CO₂-TPD results show that the Pd@HTc catalyst exhibits higher concentration of basic sites compared with that of Pd@HTc–Ac and Pd@Ac catalysts. The H₂-TPR profiles show that the reducibility of Pd species is highly dependent on the nature of the supports. Catalytic activity results reveal that the conversion of glycerol over Pd catalysts increased in the following order: Pd@Ac < Pd@HTc–Ac < Pd@HTc, while selectivity of the glyceric acid increased in the following order: Pd@HTc–Ac < Pd@Ac < Pd@HTc. The presence of more number of basic sites and high dispersion of Pd nanoparticles are found to be key factors for excellent catalytic performance of Pd@HTc catalyst in the oxidation of glycerol with molecular oxygen.

© 2016 Elsevier Ltd. All rights reserved.

1. Introduction

The negative impacts of fossil fuels on climate change, along with concerns on local economic dependencies and social sustainability have motivated the scientific community to search for alternative renewable energy sources [1,2]. In this context, biomass, one of the important renewable resources, can be used to produce valuable chemicals and fuels that are currently being produced from fossil fuels. However, only 3.5% of the existing biomass is presently being used for human needs, which includes food (around 62%), energy use, paper and construction needs (33%), and clothing, detergents and chemicals (5%). The remaining 96.5% of the biomass is used in the planetary ecosystem [3]. Therefore, the transformation of biomass to useful products still represents an emerging field that has potential to overcome the concerns of fossil fuels, however there is an urgent need to develop substantial economical routes for efficient biomass valorisation.

Bio-glycerol, one of the top 10 bio-platform chemicals estimated by the US Department of Energy, has attracted much

attention because of its high abundance and excellent functionality due to the presence of three hydroxyl molecules [2]. Glycerol can be largely obtained (~10 wt.%) during biodiesel synthesis process [1,2]. A number of catalytic processes, such as oxidation, hydrogenation, hydrogenolysis, dehydration, esterification, and transesterification have been reported to efficiently convert glycerol into valuable chemicals [4–6]. The liquid phase oxidation of glycerol is one of the most promising routes to produce high-value chemicals. As shown in Fig. 1, a number of products, such as dihydroxyacetone (DHA), glyceric acid (GLYAC), glyceraldehyde (GLYALD), hydroxypyruvic acid (HYPAC), and glycolic acid (GLYCAC) are possible in glycerol oxidation [7–10]. Among all these products, glyceric acid is an important chemical with potential applications [8,11]. For example, glyceric acid can be used for treatment of skin disorders, its ester for biodegradable fabric softener, and derivatives as building block compounds for bio-based polyesters [12].

The glycerol conversion and distribution of the products in the oxidation of glycerol are dependent on the nature of the catalyst, reaction conditions, and oxidant source [14]. The liquid phase oxidation of glycerol has been investigated using few monometallic and bimetallic catalysts based on Au, Pt, and Pd in basic medium [4,6,15–20]. Hutchings and his research group [21,22] found that

* Corresponding author.

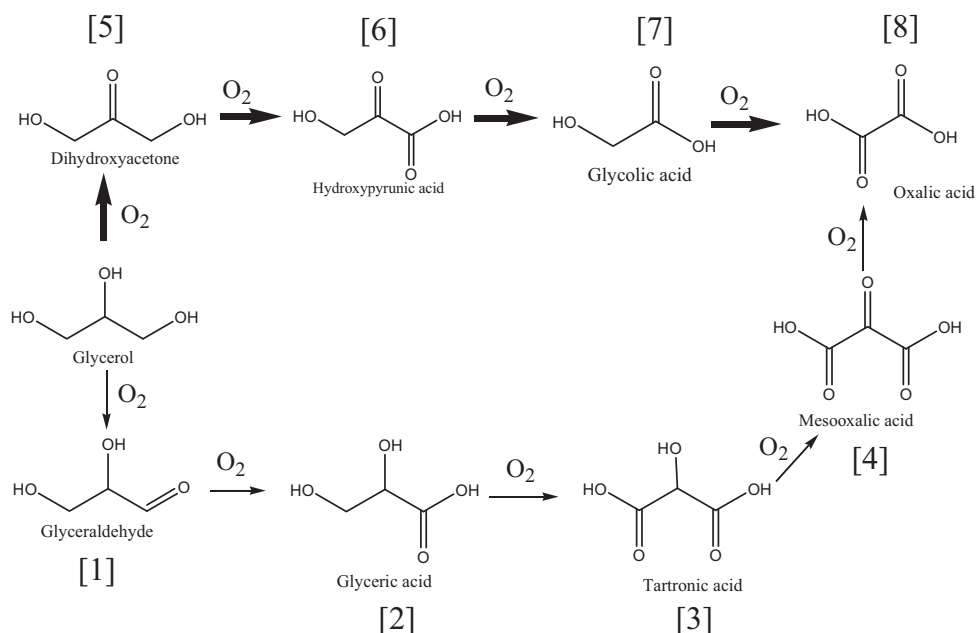


Fig. 1. General reaction pathways in liquid phase oxidation of glycerol [13].

the activity of the gold catalysts is strongly dependent on the basicity of the reaction medium. Base plays a key role in the oxidation of glycerol by abstracting hydrogen from the primary OH groups of glycerol, which is the rate limiting step in this reaction [23]. Peroxide could also be formed and contributed to the C–C bond cleavage of the glycerol during glycerol oxidation over the gold catalyst [19]. The activity of the Au catalysts on different supports, such as TiO₂, Al₂O₃, and carbon has been investigated for glycerol oxidation [8,23–26]. Among the above used supports, carbon was proven to be a better support for gold catalysts in glycerol oxidation [17,25], which is due to its high surface area and larger porosity. However, sodium glycerate is formed in alkaline solution, thus to get free glyceric acid, neutralization and acidification should be further needed [24]. As well, the high price and limited availability of gold is limiting the applications of Au-based catalysts in chemical industry. Therefore, the development of novel, efficient heterogeneous catalysts having appropriate metal active phases and supports is needed for sustainable biomass valorisation [27].

Relatively, Pd is cheap and abundant compared to Au, and it is widely used as heterogeneous and homogeneous catalytic component in many industrial applications, such as vinyl synthesis, acetylene hydrogenation, and automobile exhaust purification [28]. Blackburn et al. reported the first successful example of Pd catalyzed aerobic oxidation of secondary alcohols to produce ketones [29]. The successful oxidation reactions were also carried out with Pd nanoparticles catalyst [26–28]. Selective oxidation of glycerol to glyceric acid was performed using nanoscale Pd catalysts under base-free conditions [13]. Recently, hydrotalcites are used as efficient supports for dispersing the noble metals and their catalytic efficiency was investigated for liquid-phase oxidation of primary alcohols [30,31]. Hydrotalcites exhibit numerous catalytically favourable properties, such as high basicity, structural stability, homogeneous dispersion of active metals, and better resistance to sintering [31].

Therefore, in this work we synthesized various Pd-based catalysts supported on hydrotalcite, activated carbon, and composite of activated carbon–hydrotalcite using an immobilization method. The physicochemical properties of the catalysts were investigated using powder X-ray diffraction (XRD), N₂ adsorption–desorption,

X-ray fluorescence (XRF), H₂-temperature-programmed reduction (H₂-TPR), CO₂-temperature programmed desorption (CO₂-TPD), and transmission electron microscopy (TEM) techniques. The efficiency of the catalysts was tested for liquid-phase oxidation of glycerol with molecular oxygen. Much attention has been paid to understand the structure–activity properties of Pd catalysts in liquid phase oxidation of glycerol.

2. Experimental

2.1. Materials

Na₂PdCl₄ (99.99%) and polyvinyl alcohol (PVA, M_w = 146,000–186,000, 87–89% hydrolysed) were purchased from Sigma–Aldrich. Stock activated carbon was purchased from United Chem (surface area = 1100–1250 m² g⁻¹ and pH ~ 9–10). The other reagents used in this work are Mg(NO₃)₂·6H₂O (Merck, 99%), Al(NO₃)₃·9H₂O (Merck, 98.5%), NaOH (Merck, 99%), Na₂CO₃ (Sigma–Aldrich, 98%), and HNO₃ (Sigma–Aldrich, 70%). The oxygen was purchased from MOX–Linde (99.99%).

2.2. Catalyst preparation

2.2.1. Preparation of activated carbon (Ac) support

The crude activated carbon is treated with 5 M HNO₃ under vigorous magnetic stirring at room temperature for 24 h. The treatment was performed at 500 mL/10 g ratio of HNO₃ to carbon sample. After the treatment, the sample was filtered off and thoroughly washed with distilled water until the pH of the solution reach to ~7 [32]. Afterwards, the carbon material was over-dried at 333 K.

2.2.2. Preparation of hydrotalcite (HTC)

The hydrotalcite (Mg/Al ratio = 4) was prepared using a co-precipitation method [33]. In brief, the requisite amounts of 2.40 mol Mg(NO₃)₂·6H₂O and 0.6 mol Al(NO₃)₃·9H₂O were dissolved in 227.5 mL distilled water (solution A). The solution A was then added drop wise to another solution B, which contained

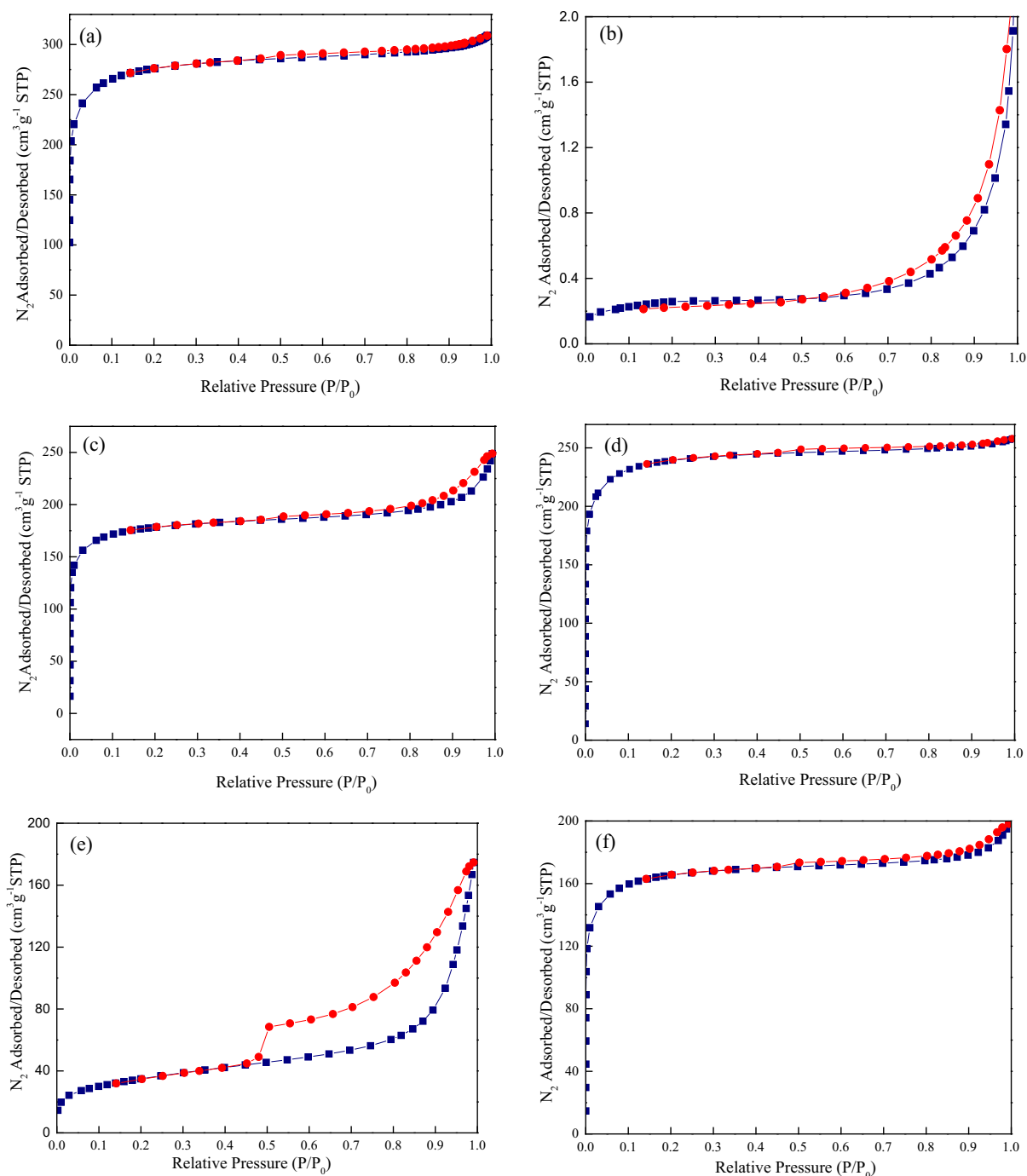


Fig. 2. N_2 adsorption/desorption isotherms of (a) Ac, (b) HTc, (c) HTc-Ac (d) Pd@Ac, (e) Pd@HTc and (f) Pd@HTc-Ac: ● desorption ■ adsorption.

Table 1
Textural properties of the supports and Pd catalysts.

Catalyst	BET surface area ($m^2 g^{-1}$)	Pore volume ($cm^3 g^{-1}$)	Pore diameter (nm)	Pd particle size (nm)	
				XRD	TEM
Ac	917.9	0.4664	3.590	–	–
HTc	126.7	0.0291	17.379	–	–
HTc-Ac	648.1	0.1444	8.644	–	–
Pd@Ac	917.1	0.0294	4.450	11.00	9.10
Pd@HTc	125.6	0.2754	7.853	8.90	9.01
Pd@HTc- Ac	632.2	0.0516	8.113	22.01	11.16

^aDetermined by XRF.

250.9 mL aq. solution of Na_2CO_3 (2 mol) and NaOH (6 mol) under vigorous stirring at room temperature. The suspension was left for 12 h at 300 K and the pH of the sol–gel solution was around 13. The sample was then filtered off and washed with distilled water until the pH of the solution reach to ~ 7 . The resultant gel was dried at 333 K overnight and calcined at 723 K in N_2 for 5 h to obtain its oxide form.

2.2.3. Preparation of activated carbon–hydrotalcite composite

The activated carbon and hydrotalcite were mixed by taking a 1:1 weight ratio to obtain the composite of activated carbon–hydrotalcite (Ac–HTc).

2.2.4. Synthesis of supported Pd catalysts

The supported Pd catalysts with 1% Pd loading were prepared using an immobilization method with polyvinyl alcohol. The Pd precursor was pre-reduced with NaBH_4 with a 2:1 M ratio of NaBH_4 :Pd (formation of dark brown sol). Within a few minutes of sol generation, the colloid was immobilized by adding support (activated carbon, hydrotalcite, and composite of hydrotalcite and activate carbon) under vigorous stirring. The slurry was stirred until all the palladium was deposited on the support. Afterwards, the sample was filtered off and dried at 333 K overnight. The catalyst was then calcined at 673 K under N_2 flow (50 mL min^{-1}) and reduced in a stream of N_2 and H_2 (90:10) at 150 mL min^{-1} flow rate for 4 h at 723 K.

2.3. Catalyst characterization

The specific surface area, pore volume, and average pore size of the catalysts were measured by N_2 adsorption–desorption technique using Micromeritics Tristar ASAP 3020 at 77 K. The Pd loadings on the surface of the catalysts were determined by XRF (S4EXPLORER, Bruker AXS). The H_2 -TPR studies were carried out using Thermofinnigan TPDRO 1100 in a fixed-bed reactor equipped with a thermal conductivity detector using 5% H_2 balance in N_2 (30 mL/min). The amount of catalyst was 50 mg and the temperature was increased from room temperature to 800 K at a heating rate 1 K min^{-1} . The CO_2 -TPD studies were conducted using Thermofinnigan TPDRO 1100. The catalyst (50 mg) was placed in a

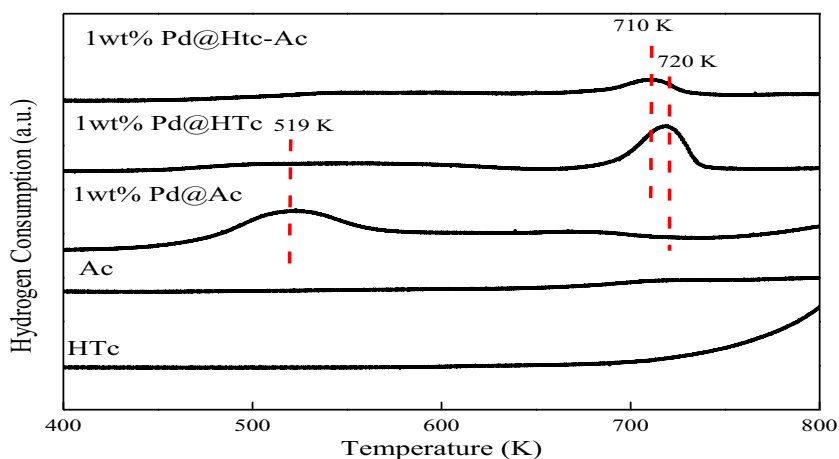


Fig. 3. H_2 -TPR profiles of the supports and corresponding Pd catalysts.

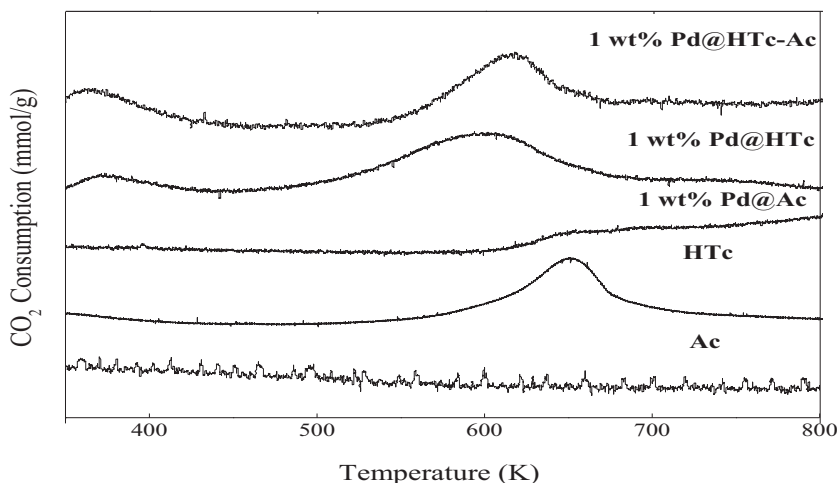


Fig. 4. CO_2 -TPD profiles of the supports and corresponding Pd catalysts.

Table 2

Liquid phase oxidation of glycerol using supports and Pd catalysts.

Catalyst	CO_2 uptake amount (mmol/g)	Conversion (%)	Selectivity (%)				TOF (h^{-1})
			DHA	GLYALD	GLYAC	TARAC	
Ac	–	<1	n.d.	n.d.	n.d.	n.d.	n.d.
HTc	2.357	<1	n.d.	n.d.	n.d.	n.d.	n.d.
Pd@Ac	0.321	51.45	11.21	13.20	57.66	17.93	125.30
Pd@HTc	1.936	70.35	n.d.	0.84	80.37	18.79	165.58
Pd@HTc-Ac	1.421	63.78	n.d.	1.46	35.18	17.56	147.47

Reaction conditions: 0.3 M glycerol solution, glycerol/Pd = 3500 mol/mol, 363 K, 1000 rpm and mole ratio of $\text{NaOH/glycerol} = 2$, O_2 pressure = 8 bar, and reaction time = 180 min, n.d: not determined.

tubular quartz sample tube and the sample was pre-treated at ambient condition under N_2 flow of 10 mL min^{-1} for 30 min. The sample was exposed to CO_2 at room temperature to the 393 K (10 K min^{-1}). Desorption was carried out from room temperature to 873 K at a heating rate of 10 K min^{-1} . The X-ray diffraction (XRD) patterns were recorded using X-ray diffractometer (Bruker) with $Cu \text{ K}\alpha$ ($\lambda = 0.154 \text{ nm}$) radiation. The particle size of the catalysts were measured by transmission electron microscope (TEM) (JEM 2100F:JEOL).

2.4. Glycerol oxidation

A batch stainless steel autoclave reactor (200 mL of Top Industries) was used for the liquid phase oxidation of glycerol. In a typical experiment, 0.3 M of glycerol with glycerol/Pd = 3500 and 2 mol ratio of NaOH/glycerol were charged into the reactor. The autoclave was purged with O_2 and then pressurized to 8 bar at room temperature. The reaction mixture was heated to 363 K for 180 min under

a stirring speed of 1000 rpm. The concentration of the reactant and products were analysed by high-performance liquid chromatography (Shimadzu HPLC) equipped with refractive index (RI) detector. An Agilent Hi-Plex H, $7.7 \times 300 \text{ mm}$, $8 \mu\text{m}$ column was employed for product separation at 338 K with 0.0085 M H_2SO_4 solution as the mobile phase flowing at 0.55 mL min^{-1} . Products were identified by comparison of HPLC standard compounds.

3. Results and discussion

3.1. Catalyst characterization

3.1.1. N_2 adsorption–desorption and elemental analyses

The N_2 adsorption–desorption isotherms of the catalysts are shown in Fig. 2. The BET surface area, pore size, and pore volume of the catalysts are presented in Table 1. The isotherm of activated carbon can be classified as type I with H_4 type hysteresis, indicating the presence of both micropores and mesopores. The

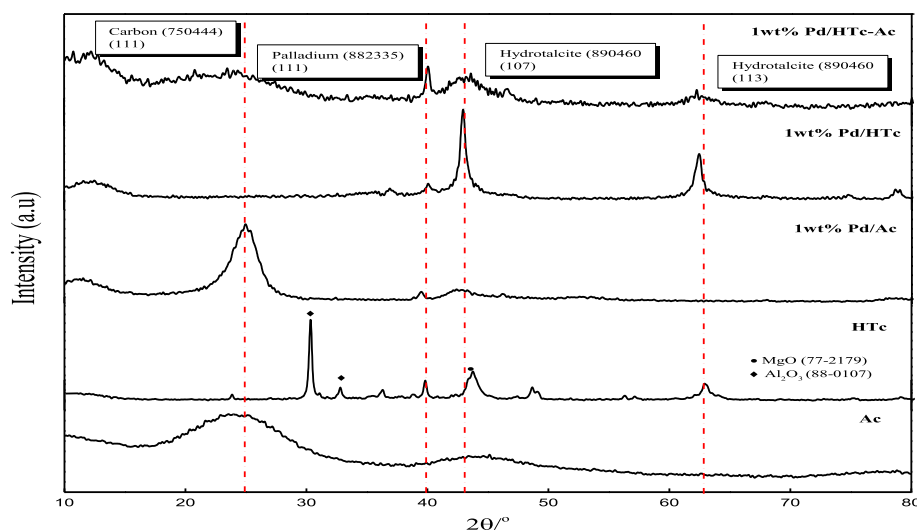


Fig. 5. Powder XRD patterns of the supports and Pd-based catalysts.

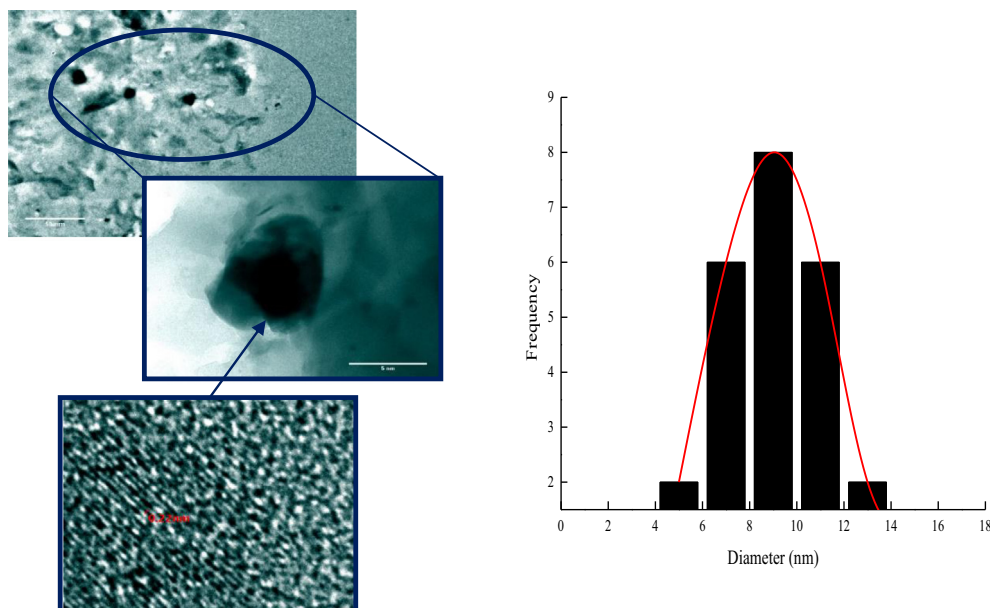


Fig. 6a. TEM overview image of Pd@HTc and palladium particle distribution.

estimated average pore diameter of Ac support is 3.59 nm (Table 1). In contrast, the HTc support exhibits type IV isotherm with H_1 type hysteresis loop and the obtained average pore diameter is 17.3 nm, confirming that HTc has mesoporous structure [34–36]. The isotherm of HTc-Ac is almost similar to Ac isotherm, i.e. type I with H_4 hysteresis type. The estimated average pore diameter of HTc-Ac is \sim 8.644 nm. There was no effect of Pd addition on the isotherm of the Ac and Ac-HTc supports: the estimated average pore diameters are 4.450 and 8.113 nm, respectively. In contrast, the addition of Pd to HTc resulted in a significant variation in shape of isotherm and the obtained pore diameter of Pd@HTc catalyst is 7.853 nm. The Pd@HTc-Ac catalyst shows type I with H_4 type hysteresis, which indicates the presence of both micropores and mesopores.

It can be noted from Table 1 that the Ac support shows high BET surface area of $917.9 \text{ m}^2 \text{ g}^{-1}$ [32]. The HTc support has low BET surface area ($126.7 \text{ m}^2 \text{ g}^{-1}$), which is improved to $648.1 \text{ m}^2 \text{ g}^{-1}$ after

the addition of Ac. Due to the relatively low Pd loadings used in this study, there was no significant variation in the specific surface area of Pd@Ac and Pd@HTc catalysts with respect to supports. However, the BET surface area of the Ac-HTc is considerably decreased from 648.1 to $632.2 \text{ m}^2 \text{ g}^{-1}$ after the addition of Pd. The XRF measurements showed that the employed method provides better Pd retention efficiencies and the determined Pd contents in Pd@Ac Pd@HTc and Pd@HTc-Ac were 1.02, 1.12, and 1.20%, respectively (Table 1).

3.1.2. H_2 -TPR studies

The H_2 -TPR profiles of the Pd catalysts, including the supports are shown in Fig. 3. As can be noted from Fig. 3, no reduction peaks were found in the case of supports. On the other hand, the Pd@Ac catalyst shows a major peak at \sim 525 K, which can be assigned to the reduction of Pd^{2+} species to metallic Pd [37]. The position of this peak is shifted to higher temperatures (\sim 715 K) for the

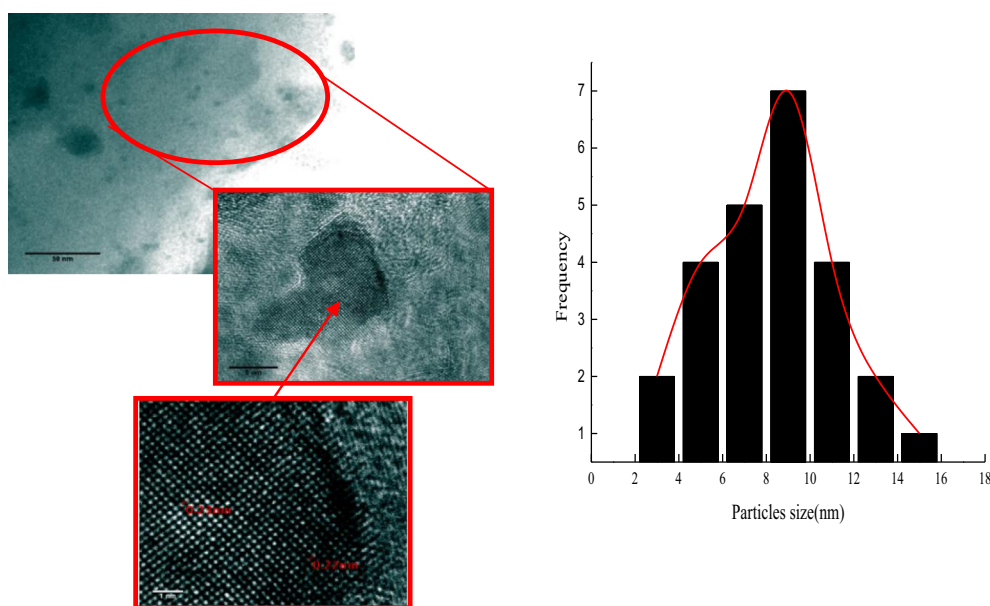


Fig. 6b. TEM overview image of Pd@Ac and palladium particle size distribution.

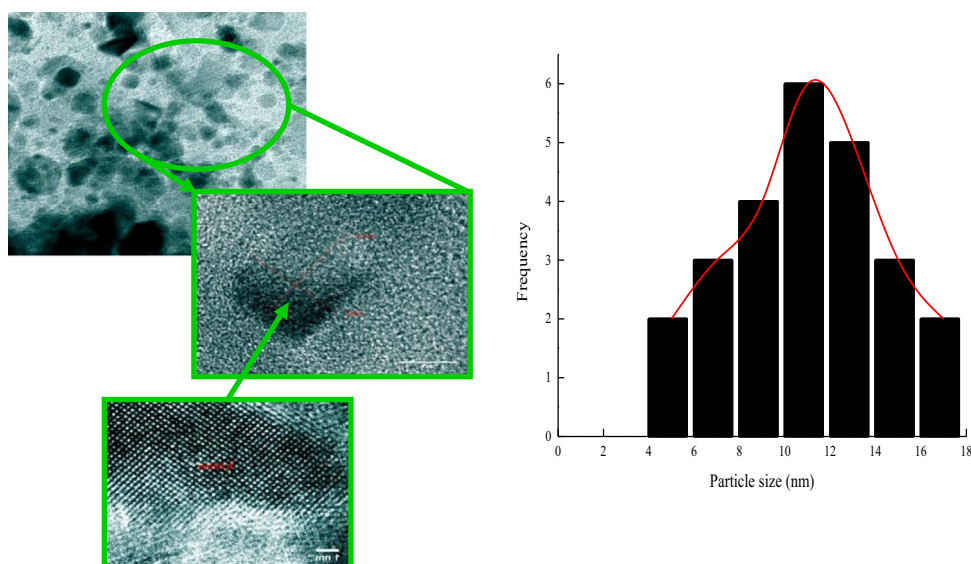


Fig. 6c. TEM overview image of Pd@HTc-Ac and palladium particle size distribution.

Pd@HTc and Pd@HTc-Ac catalysts. The presence of reduction peak at higher temperatures may be due to the strong interaction of Pd particles with support or existence of highly coordinated types, causing more resistance to reduce Pd²⁺ to Pd [37,38].

3.1.3. CO₂-TPD studies

The basic properties of the catalysts were investigated using CO₂-TPD technique (Fig. 4). No peaks were found in Ac and Pd@Ac

samples, indicating that these samples do not show any basic properties. In contrast, the HTc, Pd@HTc, and Pd@HTc-Ac samples exhibit a major peak in the range of 600–700 K. This peak indicates the presence of medium basic sites in the synthesized catalysts. The medium basic sites are related to the metallic oxygen bridge like Mg²⁺-O²⁻ and Al³⁺-O²⁻ pairs. As shown in Table 2, the Pd@HTc catalyst shows a strong ability towards CO₂ uptake compared to Pd@HTc-Ac and Pd@Ac catalysts, indicating presence of more

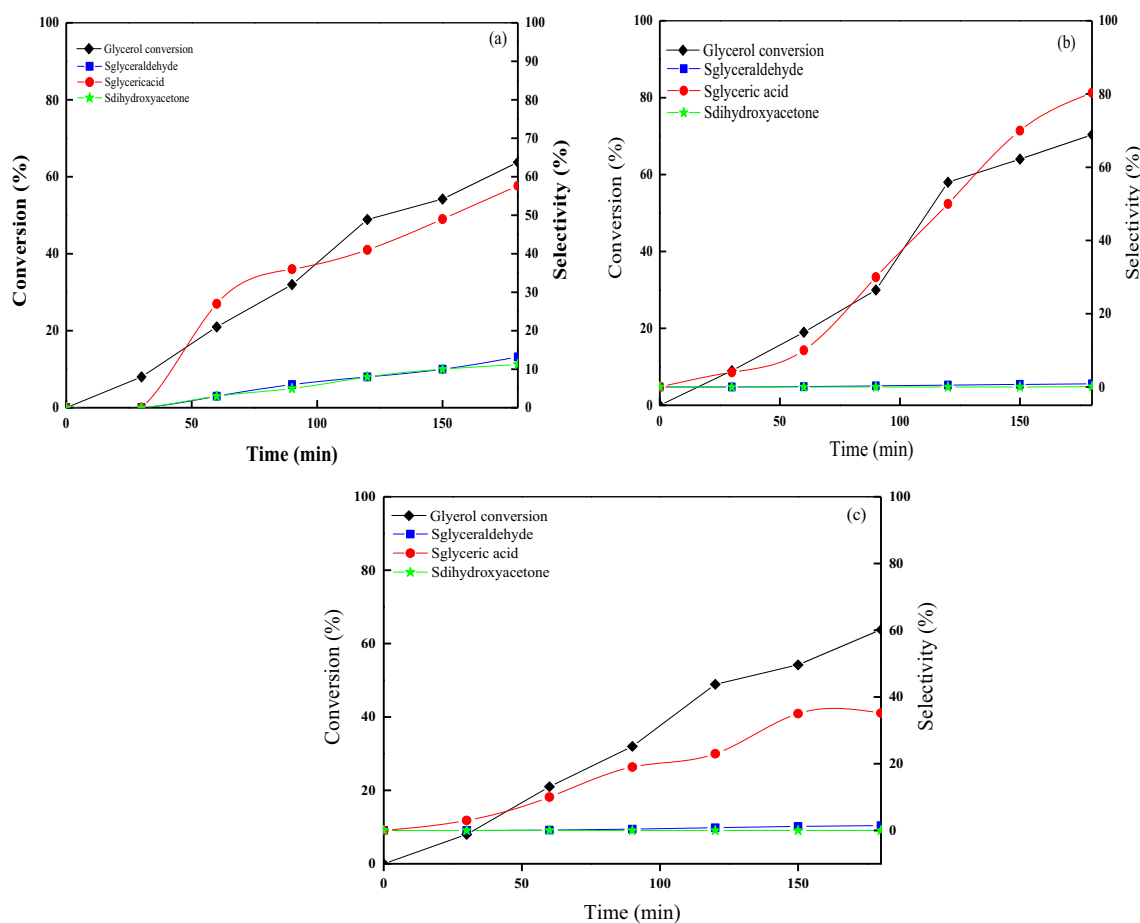


Fig. 7. Time course of glycerol oxidation over (a) Pd@Ac (b) Pd@HTc and (c) Pd@HTc-Ac catalysts.

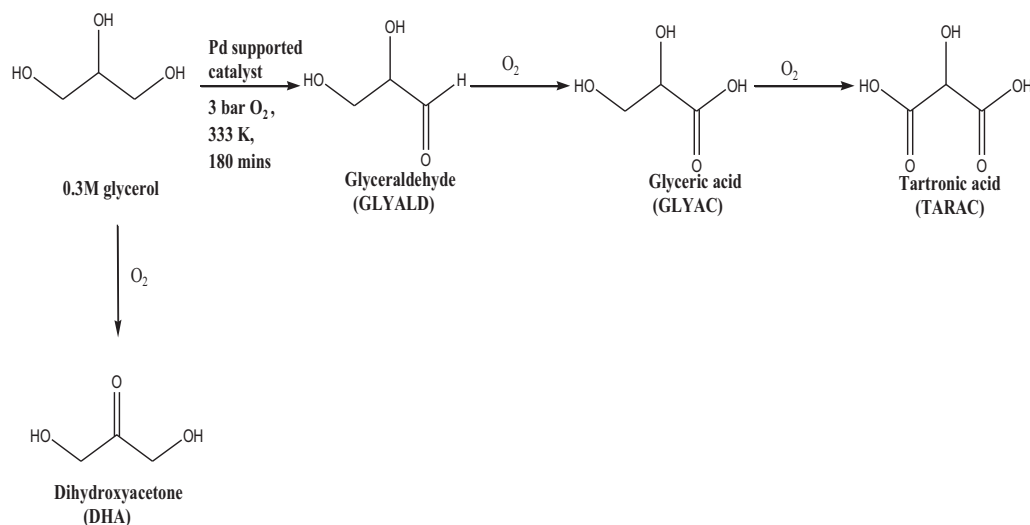


Fig. 8. Reaction pathway for liquid-phase oxidation of glycerol over Pd catalysts.

number of basic sites in Pd@HTc catalyst, which is highly beneficial for glycerol oxidation, as discussed in the activity part [38].

3.1.4. Powder XRD studies

The XRD patterns of the supports and corresponding Pd catalysts are shown in Fig. 5. The Ac support shows two peaks at 26.31 and 42.03°, which can be assigned to pure carbon and carbon oxide, respectively. This is due to the pre-treatment of HNO₃ on the carbon surface. Calcined HTc shows various reflections as shown in Fig. 5, and clearly indicates that the structure of HTc collapsed during the calcination at 773 K (PDF 89–0460). The noticed peaks at 2 theta of 29.56, 31.84, and 48.51° in HTc support indicate the presence of Al₂O₃, resulted from the impurities of the hydrotalcite (PDF 88–0107) [39]. In addition, the supported Pd catalysts show a minor peak at 40.03°, which corresponds to metallic Pd (PDF88–2335). No detectable diffraction peaks correspond to PdO crystallites were found. This is due to low concentration of PdO and/or its high dispersion on the support. However, it cannot be ruled out that the PdO crystallites might be present as smaller crystallites, which are unable to be detected by powder XRD [37]. The average Pd crystallite size of the Pd catalyst was estimated using a Scherrer equation and the data was presented in Table 1 [40]. Among the Pd catalysts, the Pd@HTc catalyst has the smallest Pd crystallites size (8.90 nm).

3.1.5. TEM studies

The particle size and morphology of the Pd catalysts were determined by TEM analysis. The TEM images of Pd@HTc-Ac, Pd@Ac, and Pd@HTc catalysts are shown in Fig. 6. A close observation of all images reveals the formation of different size of palladium particles with irregular morphologies. It is a known fact that aggregation of smaller seeds of spherical particles leads to large size nanoparticles [41]. Fitting by Log-Normal function, the particle size of Pd species was estimated and the data was presented in Fig. 6. The estimated average diameter of palladium particles is summarized in Table 1. It can be seen from Fig. 6a that the Pd@HTc catalyst has better dispersion of Pd particles with an average diameter ~9.01 nm (Table 1). In contrast, different sized particles can be found ranging from 2 to 16 and 14 to 18 nm for Pd@Ac (average diameter is ~9.10 nm) and Pd@HTc-Ac catalysts (average diameter is ~11.16 nm), respectively (Table 1).

3.1.6. Catalytic activity studies

The liquid phase oxidation of glycerol with molecular oxygen was studied using the Pd catalysts in a 200 mL autoclave vessel [42,43]. The reaction conditions used for the glycerol oxidation are 8 bar O₂, 363 K and 1000 rpm. The obtained results as a function of time are presented in Fig. 7. For comparison purpose, the catalytic efficiency of the supports was also tested for glycerol oxidation at 180 min and the results are presented in Table 2. It can be noted from Table 2 that HTc and Ac show a negligible performance in glycerol oxidation, indicating that HTc and Ac could only play a support role for dispersing the Pd catalysts. As shown in Fig. 7, the conversion of glycerol increases with the increase of time for all the Pd catalysts. Among the catalysts tested, the Pd@HTc catalyst exhibits the highest glycerol conversion of 70.35% followed by Pd@HTc-Ac (63.78%) and Pd@Ac (51.45%) (Table 2). Interestingly, the selectivity of the glyceric acid follows different trends, depending up on the catalysts. As shown in Fig. 7, the selectivity of glyceric acid is very low at initial times for Pd@Ac catalyst, which is significantly increased to 27 and 57.66% for 60 and 180 min, respectively. However, there was no much improvement in the selectivity of the glyceric acid with time in the case of Pd@HTc-Ac catalyst: the observed selectivity of the glyceric acid was 35.18% for 180 min. On the other hand, the Pd@HTc shows a prominent role in achieving higher selectivity of the glyceric acid: a 80.37% of glyceric acid was found for 180 min. Turn over frequency (TOF) values were calculated at highest conversion for each catalyst using Eq. (1). In addition to glyceric acid, various by-products, such as glyceraldehyde and dihydroxyacetone are also found as shown in Fig. 8.

$$\text{TOF} = \frac{\text{mmol of converted glycerol}}{\text{mmol of total Pd} \times \text{Reaction time (hour)}} \quad (1)$$

It is a well-known fact that the basicity of the catalysts plays a key role in the glycerol oxidation [16–18,44]. As well, a high dispersion of active phase species is needed for any heterogeneous catalytic reaction, including glycerol oxidation. It can be noted from Fig. 6 and Table 2 that the Pd@HTc catalyst has highly dispersed palladium species and more number of basic sites compared to other synthesized Pd catalysts. These improved properties are the main reasons for high catalytic performance of the Pd@HTc catalyst in glycerol oxidation (Fig. 7 and Table 2).

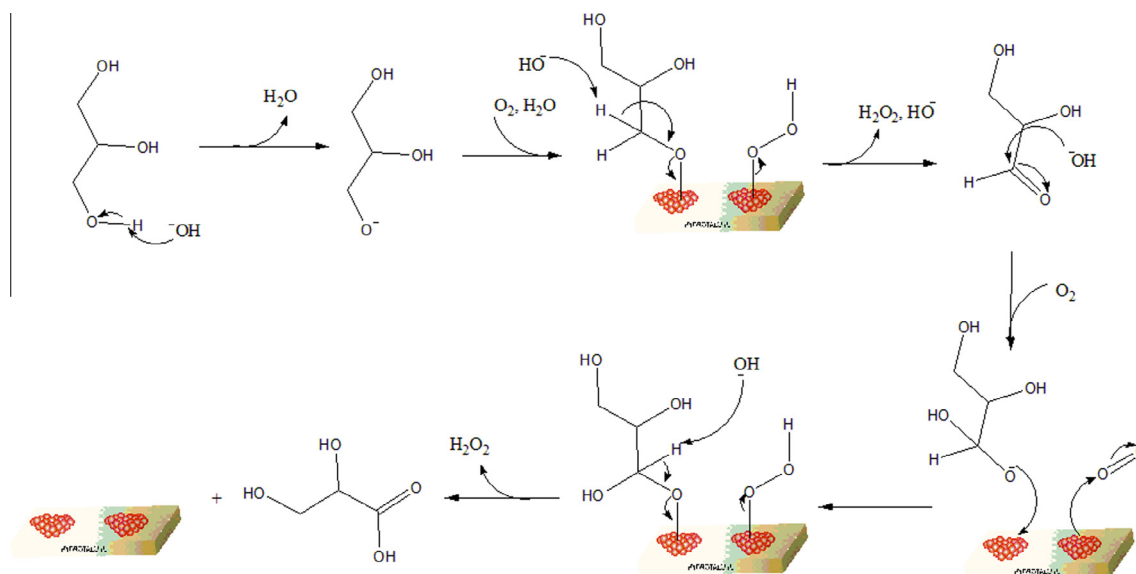


Fig. 9. Proposed mechanism of glycerol oxidation over Pd@HTc catalyst.

3.1.7. Proposed reaction mechanism

Based on the results obtained in this study and previously reported literature [19,44,45], we proposed a reaction pathway for the oxidation of glycerol to glyceric acid as shown in Fig. 9. First step is abstraction of the hydroxyl hydrogen of the glycerol by a base, giving a alkoxide [46]. The formed alkoxide reacts with OH^- , formed by the dissociation of molecular oxygen on Pd species, cation of O_2 with water and from base catalyst on palladium sites and form intermediate. The partially oxygenated intermediate isomerizes on palladium hydride species to give glyceric acid. This palladium hydride will spontaneously react with molecular oxygen, followed by pre-adsorption step and removal of the palladium hydroxide by proton to form water while recovering the initial metallic state. The rate-determining step is the abstraction of the hydrogen from alcohol group [47]. The 1 wt%Pd@HTc catalyst exhibit high dispersed smaller Pd particles and high concentration of basic sites, thus better performance in glycerol oxidation giving higher glycerol conversion and superior selectivity of glycerol carbonate.

4. Conclusions

In summary, the liquid phase oxidation of glycerol was investigated using Pd-based catalysts synthesized by an immobilization method. TEM studies reveal that Pd particles are well dispersed on the surface of the supports, mainly on HTc support. The reducibility of the PdO is highly dependent on the nature of the supports. The CO_2 -TPD results show that the Pd@HTc catalyst exhibits more number of basic sites compared to Pd@HTc-Ac and Pd@Ac catalysts. Among the catalysts tested, the Pd@HTc catalyst showed excellent performance in terms of higher glycerol conversion and superior selectivity of glyceric acid. In contrast, negligible glycerol conversions were found in the case of supports. The catalytic performance of the Pd/HTc catalyst is mainly attributed to higher amounts of basic sites and well dispersion of Pd nanoparticles.

Acknowledgments

The authors express sincere gratitude to Nanocat, University of Malaya technical service team for their service contribution in samples characterization. Our thanks also go to MOE HIR Grant (F00032) for financial support.

References

- [1] P. Sudarsanam, B. Malleshham, A.N. Prasad, P.S. Reddy, B.M. Reddy, Synthesis of bio-additive fuels from acetalization of glycerol with benzaldehyde over molybdenum promoted green solid acid catalysts, *Fuel Process. Technol.* 106 (2013) 539–545.
- [2] B. Malleshham, P. Sudarsanam, B.V.S. Reddy, B.M. Reddy, Development of cerium promoted copper–magnesium catalysts for biomass valorization: selective hydrogenolysis of bioglycerol, *Appl. Catal. B: Environ.* 181 (2016) 47–57.
- [3] C. Chan-Thaw, S. Campisi, D. Wang, L. Prati, A. Villa, Selective oxidation of raw glycerol using supported AuPd nanoparticles, *Catalysts* 5 (2015) 131.
- [4] D. Liang, J. Gao, J. Wang, P. Chen, Y. Wei, Z. Hou, Bimetallic Pt–Cu catalysts for glycerol oxidation with oxygen in a base-free aqueous solution, *Catal. Commun.* 12 (2011) 1059–1062.
- [5] J.J. Bozell, G.R. Petersen, Technology development for the production of biobased products from biorefinery carbohydrates—the US Department of Energy's "Top 10" revisited, *Green Chem.* 12 (2010) 539.
- [6] D. Liang, S. Cui, J. Gao, J. Wang, P. Chen, Z. Hou, Glycerol oxidation with oxygen over bimetallic Pt–Bi catalysts under atmospheric pressure, *Chin. J. Catal.* 32 (2011) 1831–1837.
- [7] M.-C. Daniel, D. Astruc, Gold nanoparticles: assembly, supramolecular chemistry, quantum-size-related properties, and applications toward biology, catalysis, and nanotechnology, *Chem. Rev.* 104 (2004) 54.
- [8] S. Carrettin, P. McMorn, P. Johnston, K. Griffin, C.J. Kiely, G.A. Attard, G.J. Hutchings, Oxidation of glycerol using supported gold catalysts, *Top. Catal.* 27 (2004) 6.
- [9] N. Dimitratos, A. Villa, L. Prati, Liquid phase oxidation of glycerol using a single phase (Au–Pd) alloy supported on activated carbon: effect of reaction conditions, *Catal. Lett.* 133 (2009) 334–340.
- [10] N. Dimitratos, F. Porta, L. Prati, Au, Pd (mono and bimetallic) catalysts supported on graphite using the immobilisation method, *Appl. Catal. A: Gen.* 291 (2005) 210–214.
- [11] M. Pagliaro, R. Ciriminna, H. Kimura, M. Rossi, C. Della Pina, From glycerol to value-added products, *Angew. Chem., Int. Ed.* 46 (2007) 4434–4440.
- [12] C.S. Hong, S.Y. Chin, C.K. Cheng, M.M. Sabri, G.K. Chua, Enzymatic conversion of glycerol to glyceric acid with immobilised laccase in Na-alginate matrix, *Procedia Chem.* 16 (2015) 632–639.
- [13] S. Carrettin, P. McMorn, P. Johnston, K. Griffin, C.J. Kiely, G.J. Hutchings, Oxidation of glycerol using supported Pt, Pd and Au catalysts, *Phys. Chem. Chem. Phys.* 5 (2003) 1329–1336.
- [14] A. Villa, G.M. Veith, L. Prati, Selective oxidation of glycerol under acidic conditions using gold catalysts, *Angew. Chem., Int. Ed.* 49 (2010) 4499–4502.
- [15] E.G. Rodrigues, S.A.C. Carabineiro, J.J. Delgado, X. Chen, M.F.R. Pereira, J.J.M. Órfaõ, Gold supported on carbon nanotubes for the selective oxidation of glycerol, *J. Catal.* 285 (2012) 83–91.
- [16] G.L. Brett, Q. He, C. Hammond, P.J. Miedzkiak, N. Dimitratos, M. Sankar, A.A. Herzing, M. Conte, J.A. Lopez-Sanchez, C.J. Kiely, D.W. Knight, S.H. Taylor, G.J. Hutchings, Selective oxidation of glycerol by highly active bimetallic catalysts at ambient temperature under base-free conditions, *Angew. Chem., Int. Ed.* 50 (2011) 10136–10139.
- [17] S. Gil, M. Marchena, L. Sánchez-Silva, A. Romero, P. Sánchez, J.L. Valverde, Effect of the operation conditions on the selective oxidation of glycerol with catalysts based on Au supported on carbonaceous materials, *Chem. Eng. J.* 178 (2011) 423–435.
- [18] A. Villa, D. Wang, G.M. Veith, L. Prati, Bismuth as a modifier of Au–Pd catalyst: enhancing selectivity in alcohol oxidation by suppressing parallel reaction, *J. Catal.* 292 (2012) 73–80.
- [19] B.N. Zope, S.E. Davis, R.J. Davis, Influence of reaction conditions on diacid formation during Au-catalyzed oxidation of glycerol and hydroxymethylfurfural, *Top. Catal.* 55 (2012) 24–32.
- [20] D.M. Alonso, S.G. Wettstein, J.A. Dumesic, Bimetallic catalysts for upgrading of biomass to fuels and chemicals, *Chem. Soc. Rev.* 41 (2012) 8075–8098.
- [21] A.S. Hashmi, G.J. Hutchings, Gold catalysis, *Angew. Chem., Int. Ed. Engl.* 45 (2006) 7896–7936.
- [22] N. Dimitratos, A. Villa, C.L. Bianchi, L. Prati, M. Makkee, Gold on titania: Effect of preparation method in the liquid phase oxidation, *Appl. Catal. A: Gen.* 311 (2006) 185–192.
- [23] S. Gil, N. Cuenca, A. Romero, J.L. Valverde, L. Sánchez-Silva, Optimization of the synthesis procedure of microparticles containing gold for the selective oxidation of glycerol, *Appl. Catal. A: Gen.* 472 (2014) 11–20.
- [24] S. Demirel-Gülen, M. Lucas, P. Claus, Liquid phase oxidation of glycerol over carbon supported gold catalysts, *Catal. Today* 102–103 (2005) 166–172.
- [25] N. Worz, A. Brandner, P. Claus, Platinum–Bismuth-Catalyzed Oxidation of Glycerol: Kinetics and the Origin of Selective Deactivation, *J. Phys. Chem. C* 114 (2010) 1164–1172.
- [26] B. Katryniok, H. Kimura, E. Skrzyńska, J.-S. Girardon, P. Fongarland, M. Capron, R. Ducoulombier, N. Mimura, S. Paul, F. Dumeignil, Selective catalytic oxidation of glycerol: perspectives for high value chemicals, *Green Chem.* 13 (2011) 1960.
- [27] M.A. Nowak, K. Sigmund, Biodiversity: bacterial game dynamics, *Nature* 418 (2002) 138–139.
- [28] T.F. Blackburn, J. Schwartz, Homogeneous catalytic oxidation of secondary alcohols to ketones by molecular oxygen under mild conditions, *J. Chem. Soc., Chem. Commun.* (1977) 157–158.
- [29] K. Musialska, E. Finocchio, I. Sobczak, G. Busca, R. Wojcieszak, E. Gaigneaux, M. Ziolk, Characterization of alumina- and niobia-supported gold catalysts used for oxidation of glycerol, *Appl. Catal. A: Gen.* 384 (2010) 70–77.
- [30] F. Prinetto, M. Manzoli, G. Ghiotti, M.d.J. Martinez Ortiz, D. Tichit, B. Coq, Pd/Mg(Al)O catalysts obtained from hydrotalcites: investigation of acid–base properties and nature of Pd phases, *J. Catal.* 222 (2004) 238–249.
- [31] S.E. Davis, M.S. Ide, R.J. Davis, Selective oxidation of alcohols and aldehydes over supported metal nanoparticles, *Green Chem.* 15 (2013) 17–45.
- [32] J.-P. Tessonnier, D. Rosenthal, T.W. Hansen, C. Hess, M.E. Schuster, R. Blume, F. Girgsdies, N. Pfänder, O. Timpe, D.S. Su, R. Schlögl, Analysis of the structure and chemical properties of some commercial carbon nanostructures, *Carbon* 47 (2009) 1779–1798.
- [33] A. Corma, S. Hamid, S. Iborra, A. Velty, Lewis and Brønsted basic active sites on solid catalysts and their role in the synthesis of monoglycerides, *J. Catal.* 234 (2005) 340–347.
- [34] F. Cavani, F. Trifiro, A. Vaccari, Hydrotalcite-type anionic clays: preparation, properties and application, *Catal. Today* 11 (1991) 129.
- [35] Z. Wang, P. Lu, X. Zhang, L. Wang, Q. Li, Z. Zhang, NOx storage and soot combustion over well-dispersed mesoporous mixed oxides via hydrotalcite-like precursors, *RSC Adv.* 5 (2015) 52743–52753.
- [36] P. Sudarsanam, P.R. Selvakannan, S.K. Soni, S.K. Bhargava, B.M. Reddy, Structural evaluation and catalytic performance of nano-Au supported on nanocrystalline $\text{Ce}_{0.9}\text{Fe}_{0.1}\text{O}_{2-\delta}$ solid solution for oxidation of carbon monoxide and benzylamine, *RSC Adv.* 4 (2014) 43460–43469.
- [37] D. Naresh, V.P. Kumar, M. Harisekhar, N. Nagaraju, B. Putrakumar, K.V.R. Chary, Characterization and functionalities of Pd/hydrotalcite catalysts, *Appl. Surf. Sci.* 314 (2014) 199–207.

- [38] V.K. Díez, C.R. Apesteguía, J.I. Di Cosimo, Acid-base properties and active site requirements for elimination reactions on alkali-promoted MgO catalysts, *Catal. Today* 63 (2000) 53–62.
- [39] A. Tsuji, K.T. Rao, S. Nishimura, A. Takagaki, K. Ebitani, Selective oxidation of glycerol by using a hydrotalcite-supported platinum catalyst under atmospheric oxygen pressure in water, *ChemSusChem* 4 (2011) 542–548.
- [40] P. Sudarsanam, M.H. Amin, B.M. Reddy, A. Nafady, K.A. Al Farhan, S.K. Bhargava, MnOx nanoparticle-dispersed CeO₂ nanocubes: a remarkable heteronanostructured system with unusual structural characteristics and superior catalytic performance, *ACS Appl. Mater. Interfaces* 7 (2015) 16525–16535.
- [41] P. Sudarsanam, B. Hillary, D.K. Deepa, M.H. Amin, B. Mallesham, B.M. Reddy, S. K. Bhargava, Highly efficient cerium dioxide nanocube-based catalysts for low temperature diesel soot oxidation: the cooperative effect of cerium- and cobalt-oxides, *Catal. Sci. Technol.* 5 (2015) 3496–3500.
- [42] V.L. Nguyen, D.C. Nguyen, H. Hirata, M. Ohtaki, T. Hayakawa, M. Nogami, Chemical synthesis and characterization of palladium nanoparticles, *Adv. Nat. Sci. Nanosci. Nanotechnol.* 1 (2010) 035012.
- [43] N. Kakiuchi, Y. Maeda, T. Nishimura, S. Uemura, Pd(II)-hydrotalcite-catalyzed oxidation of alcohols to aldehydes and ketones using atmospheric pressure of air, *J. Org. Chem.* 66 (2001) 6620–6625.
- [44] T. Nishimura, N. Kakiuchi, M. Inoue, S. Uemura, Palladium(ii)-supported hydrotalcite as a catalyst for selective oxidation of alcohols using molecular oxygen, *Chem. Commun.* (2000) 1245–1246.
- [45] S. Chornaja, K. Dubencov, V. Kampars, O. Stepanova, S. Zhizhkun, V. Serga, L. Kulikova, Oxidation of glycerol with oxygen in alkaline aqueous solutions in the presence of supported palladium catalysts prepared by the extractive-pyrolytic method, *React. Kinet. Mech. Catal.* 108 (2012) 341–357.
- [46] T. Mallat, A. Baiker, Oxidation of alcohols with molecular oxygen on solid catalysts, *Chem. Rev.* 104 (2004) 3037–3058.
- [47] S. Hirasawa, H. Watanabe, T. Kizuka, Y. Nakagawa, K. Tomishige, Performance, structure and mechanism of Pd–Ag alloy catalyst for selective oxidation of glycerol to dihydroxyacetone, *J. Catal.* 300 (2013) 205–216.